

Chemical doping-induced gap opening and spin polarization in graphene

I. Zanella,¹ S. Guerini,² S. B. Fagan,³ J. Mendes Filho,¹ and A. G. Souza Filho^{1,*}

¹*Departamento de Física, Universidade Federal do Ceará, Caixa Postal 6030, Fortaleza, Ceará CEP 60455-900, Brazil*

²*Departamento de Física, Universidade Federal do Maranhão, São Luis, Maranhão 65080-040, Brazil*

³*Área de Ciências Naturais e Tecnológicas, Centro Universitário Franciscano, Santa Maria, Rio Grande do Sul CEP 97010-032, Brazil*

(Received 14 November 2007; revised manuscript received 19 December 2007; published 20 February 2008)

The structural and electronic properties of CrO₃ interacting with graphene layer are calculated using *ab initio* methods based on the density functional theory. The CrO₃ acts as an electron acceptor modifying the original electronic and magnetic properties of the graphene surface through an adsorption process. The changes induced in the electronic properties are strongly dependent on the CrO₃ adsorption site, and for some sites, it is possible to open a gap in the electronic band structure. Spin polarization effects are also predicted for some adsorption configurations for which the binding energy is lower and charge transfer is higher.

DOI: [10.1103/PhysRevB.77.073404](https://doi.org/10.1103/PhysRevB.77.073404)

PACS number(s): 73.22.-f, 71.15.Mb, 72.25.-b

Nanostructured carbon-based materials exhibit remarkable electronic properties making them promising materials to be used in a wide range of technological applications, including a possible carbon-based electronics in a near future.¹ Graphene, a single atom thick layer, is considered the mother structure of all *sp*² nanostructured carbon (such as fullerenes, carbon nanotubes, and ribbons), and its electronic structure has been theoretically investigated since 1947.² A breakthrough in carbon science was the recent observation of graphene single layer that was obtained by micro-mechanical cleavage of graphite.^{3,4} The linear electronic band structure at the corner of the Brillouin zone where there is a band crossing between the conduction and valence bands is responsible for striking physical properties, such as ballistic transport,⁴ and quantum Hall effect at room temperature^{5,6} and typical relativistic phenomena, such as Berry's phase and Klein paradox, as a consequence of massless Dirac fermions. The chemical stability, scalability, and the complete compatibility of graphene with current semiconductor technology pave the way for the next generation of devices operating with a carbon-based electronic.

The possibility of tailoring the electronic properties (type and number of carriers) of graphene is important not only for basic studies but also for further optimization of their applications mainly as nanoscale based sensors or spin filter devices.⁷⁻¹¹ The electronic properties can be tuned either by carrying out donor and/or acceptor doping experiments or by applying a gate bias voltage.^{9,12} The electric field polarization and the electronegativity of the doping species modify the carrier type (electron or hole) and carrier concentration at the Dirac point affecting the electronic structure and consequently the transport properties of graphene to a large extent. In this regard, a recent experimental work by Schedin *et al.*⁹ fabricated and operated a single molecule based sensor. The authors show, through measurements of quantum Hall effect, that NO₂, H₂O, and iodine act as electron acceptors whereas NH₃, CO, and ethanol present electron donor behavior on the graphene surface. These results were recently confirmed through theoretical calculations.¹³ It has also been suggested that different from normal semiconductors, doping in graphene is strongly dependent on the magnetic moment of the adsorbates.¹² These predictions point out to an interesting relationship between local magnetic moments and doping ef-

fects. Therefore, by studying the doping species in a controlled way, it is possible to access how specific chemical species perturb the graphene electronic band structure and how this impacts their physical properties such as magneto-optical and transport behavior.^{9,11} In addition, the minimum conductivity problem in graphene is a typical phenomenon of zero band gap electronic structure, and this has introduced drawbacks for developing a graphene-based electronics. Carbon ribbons have been proposed as one of the solutions for the minimum conductivity problem because, in general, its band structure exhibits a gap.^{14,15} The gap engineering can also be achieved through doping (covalent functionalization) the graphene layer with chemical species¹⁶ since the doping can induce a gap opening because of the A-B sublattice symmetry breaking. Therefore, the gap engineering in graphene is a hot topic and this has been exploited either by changing the geometry of ribbons or by interaction with substrate.^{14,17} The possibility to induce a gap in graphene through chemical doping has not yet been exploited.

In this work, the electronic properties of a single graphene layer interacting with CrO₃ molecules are analyzed through *ab initio* based calculations, and we predict that it is possible to get both gap opening and spin polarization by this functionalization process. A single graphene layer is a unique system regarding the surface to volume ratio because it is solely surface and this opens up the possibility of using CrO₃ intercalated graphene systems for the oxidation of primary alcohols. Our calculations shown that CrO₃ molecule (a model for strongly oxidizing molecules) chemically binds to graphene surface and the electronic properties of the original graphene are modified by charge transfer from graphene to this molecule leading the CrO₃ molecule acts as an electron acceptor with a similar behavior observed and predicted for CrO₃ interacting with single-wall carbon nanotubes (SWNTs).¹⁸ The effect of curvature on the adsorption of this molecule on carbon hexagonal lattice is also discussed.

First principles density functional theory has been employed to investigate electronic and structural properties of graphene interacting with CrO₃ molecule.¹⁹ The SIESTA code is used,^{20,21} which performs fully self-consistent calculations solving the spin polarized Kohn-Sham equations.²² For the exchange and correlation terms, generalized gradient approximation with the parametrization of Perdew *et al.* is

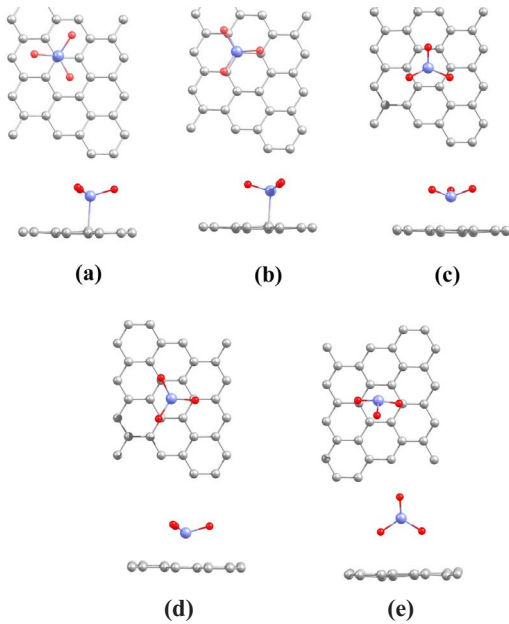


FIG. 1. (Color online) Top and side views of the most stable configurations for the CrO_3 interacting with graphene layer.

used.²³ The interaction between ionic cores and valence electrons is described by norm conserving pseudopotentials²⁴ in the Kleinman-Bylander form.²⁵ The Kohn-Sham orbitals are represented with a linear combination of pseudoatomic orbitals with a double zeta basis set plus polarization function.²¹ A cutoff of 200 Ry for the grid integration is used to represent the charge density. A $5 \times 5 \times 1$ Monkhorst-Pack grid is employed for the Brillouin zone integration,²⁶ which was shown to represent correctly their properties for the present system.²⁷

The periodic boundary conditions and a supercell approximation are used. The supercell has 32 carbon atoms for a single graphene surface in a hexagonal lattice. The structural optimizations were performed using a conjugated gradient procedure, and atomic positions of the structure are relaxed until all the force components are smaller than $0.05 \text{ eV}/\text{\AA}$.

Different configurations of CrO_3 adsorption to the graphene layer were considered in our calculations, and the most stable arrangements are shown (top and side views) in Figs. 1(a)–1(e). The configuration shown in Fig. 1(a) was predicted to be the most stable, with a Cr-C distance of about

2.32 \AA , while in the configuration shown in Fig. 1(e), the O-C bond length is about 2.95 \AA . In Table I, we list the closest distances of Cr-C and O-C for different configurations shown in Fig. 1.

The binding energies (E_B) for the studied systems are calculated using the basis set superposition error.²⁸ This correction is done through the counterpoise method using “ghost” atoms, as the following equation:

$$E_B = - [E_T(\text{graphene} + \text{CrO}_3) - E_T(\text{graphene}_{\text{ghost}} + \text{CrO}_3) - E_T(\text{graphene} + (\text{CrO}_3)_{\text{ghost}})], \quad (1)$$

where $E_T(\text{graphene} + \text{CrO}_3)$ is the total energy of the system. The ghost molecule and/or graphene corresponds to additional basis wave functions centered at the position of the CrO_3 molecule or the single layer graphene, but without any atomic potential.

The binding energies obtained for the different adsorption sites of CrO_3 on the graphene surface are listed in Table I. These results pointed out to either a physical or chemical interaction between CrO_3 and graphene, which are strongly dependent on the interaction site. For comparison sake, we also calculated the binding energy for the configuration shown in Fig. 1(a) with local density approximation (LDA) as parametrized by Ceperley and Alder,²⁹ and we obtained 2.36 eV . This upper bond value is expected since LDA is a well-known methodology which overestimates the binding energies. The transition metal atom (Cr) is preferentially bonded to the carbon atom of the graphene layer promoting an sp^3 -like hybridization (there is a small bump of 0.1 \AA of the carbon atom from the graphene surface). The Mlliken population was analyzed and used for all studied configurations to predict the electronic charge transfer from the graphene surface to the CrO_3 molecule. The graphene carbon atoms donate $0.17e$ and $0.20e$ to the CrO_3 molecule for the configurations of Fig. 1(a) and Fig. 1(e), respectively. The charge transfer on these cases occurs due to the chemical or physical adsorption of the Cr or O atoms with the carbon atoms of the graphene layer as observed on the binding energy values. We should point out that the Mlliken population does not supply a trustworthy number to charge transfer, but it indicates the trend and correct order of the charge transfer process. Then, the CrO_3 molecule behaves as an electron acceptor when interacting with the graphene layer similar to what was observed for CrO_3 adsorption on SWNT surface.¹⁸

TABLE I. Binding energies (E_B), minimal distances, and charge transfer calculated for different adsorption sites of CrO_3 on graphene layer, as shown in Fig. 1. The minus sign in the charge transfer values indicates that the CrO_3 molecule receive electronic charge.

Configuration from Fig. 1	E_B (eV)	$d(\text{Cr-C})$ (Å)	$d(\text{O-C})$ (Å)	Charge transfer to CrO_3 (e)	Electronic configuration
(a)	1.01	2.32	...	-0.17	Semiconducting
(b)	0.91	2.33	...	-0.15	Semiconducting
(c)	0.56	2.80	...	-0.11	Semimetal
(d)	0.49	2.82	...	-0.10	Semimetal
(e)	0.25	...	2.95	-0.20	Metal

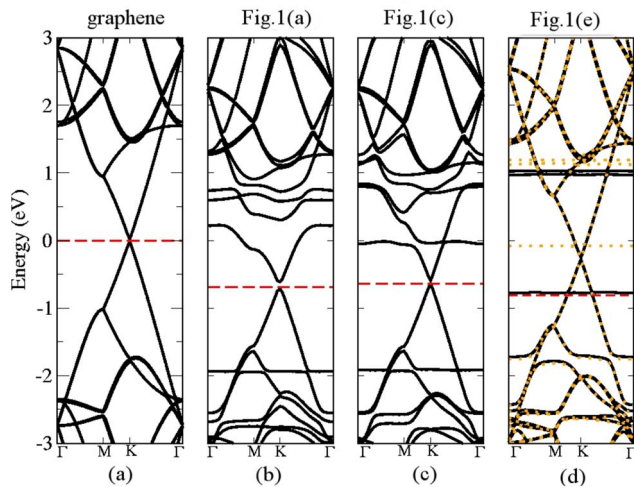


FIG. 2. (Color online) Electronic band structures for (a) pristine and for [(b), (c), and (d)] different configurations of CrO_3 adsorbed on graphene single layer, which correspond to the configurations shown in Figs. 1(a), 1(c), and 1(e), respectively. The (d) case has the filled and dotted lines corresponding, respectively, to the majority and minority spin levels. The horizontal dashed lines correspond to the Fermi energy.

The calculated electronic band structures are presented for the pristine single graphene layer [Fig. 2(a)] and for CrO_3 adsorbed on graphene [Figs. 2(b)–2(d)] in the most stable configurations shown in Figs. 1(a), 1(c), and 1(e). It is clear that the CrO_3 adsorption sites and orientation of the molecules affect the electronic properties of graphene being more pronounced for the adsorption sites shown in Fig. 1(a). The binding of CrO_3 molecule lifts the degeneracy of the band crossing close to the Fermi level, thus inducing a gap opening of about 0.12 eV at the Dirac point, which connects the valence and conduction bands at the zone edge. This gap opening is due to the breaking of graphene mirror symmetry which breaks the A-B sublattice symmetry. In order to observe this gap opening, it is need to functionalize only one sublattice. For the configuration shown in Fig. 1(b), the electronic behavior is similar to Fig. 2(b). In contrast, for the other configurations [Figs. 1(c)–1(e)], the band crossing is preserved leaving the system semimetal at 0 K. For the [Fig. 1(c)] configuration, the system remains metallic [see Fig. 2(c)], with dispersionless levels of the CrO_3 molecule on the valence and conduction bands. In this case [Fig. 2(d)], the majority (solid lines) and minority (dotted lines) carriers coming from Cr $3d$ levels are nondegenerated and located on the valence and conduction bands. Compared with the adsorption, we observe that the most stable adsorption site changes the electronic properties due to the strong hybridization between the molecule and graphene levels. It is also interesting to observe the downshift of the Fermi level resulting from the charge transfer from the graphene to the CrO_3 molecule. These shifts relative to the pristine graphene are approximately 0.69, 0.64, and 0.8 eV shown in Figs. 2(b), 2(c), and 2(d), respectively. From all the studied configurations, only the site with the CrO_3 adsorbed on the graphene surface, as shown in Fig. 1(e), presents spin polarization of

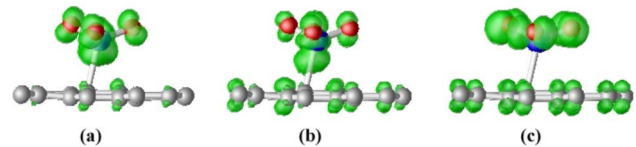


FIG. 3. (Color online) Plots for the charge isosurface of the CrO_3 interacting with graphene. The plots are for the electronic configuration presented in Fig. 2(b), located around (a) 0.8 eV, (b) -1.2 eV, and (c) -1.8 eV.

$0.4\mu_B$. This spin polarization can be understood in terms of redistribution of the electronic charge due to the interaction of the O atoms of the CrO_3 molecule and the graphene surface. In this case, a flat electronic level is located near the Fermi level [Fig. 2(d)], which is characteristic of the CrO_3 molecule.

We should point out that the splitting in majority and minority levels is a consequence that local magnetic moment occurs for the less interacting system in terms of binding energies. However, this configuration is the one that presents larger charge transfer effects thus suggesting that magnetism plays a crucial role in doping level.¹²

In Figs. 3(a), 3(b), and 3(c), the plots for the localized density of states (LDOS) of CrO_3 adsorbed on the graphene surface for the most stable configuration [shown in Fig. 1(a)] are presented for the electronic levels located about 0.8, -1.2 , and -1.8 eV, respectively. From these LDOS plots, we observe the hybridization of the molecule levels with the carbon levels from the graphene layer. This hybridization state is reflected in both binding energies and charge transfer values.

By comparing the adsorption of the CrO_3 molecule on graphene with adsorption on (8,0) SWNT surfaces,¹⁸ it is observed that the curvature effect is a crucial point to increase the adsorption of CrO_3 on the carbon hexagonal lattice. The binding energy increases by 0.4 eV for the molecule adsorbed on the inner or outer surface of the nanotube (1.4 eV for both configurations) compared with the most stable configuration on the graphene surface (1.01 eV). This effect is relevant when it is considered the real curved configuration (ripples) of the graphene layers,⁷ which will increase the efficiency of the molecule adsorption on the hexagonal carbon structures depending of the local curvature parameters.

In summary, the electronic properties of the CrO_3 molecule adsorbed on the graphene single layer were analyzed through first principles calculations. It is observed that the electronic properties and the charge transfer process are very sensitive to the CrO_3 adsorption site and also to the orientation of the molecule. This behavior is different from what was predicted by Leenaerts *et al.*¹³ for other molecules, where the interaction is not very sensitive to the adsorption site being only dependent on the molecule orientation with respect to the graphene surface. The CrO_3 molecule interacts through a chemisorption or physisorption regime on the graphene surface depending on the adsorption site, indicating

possible routes for using doped graphene layer as platform for carbon-based electronics since it is possible to engineer the gap and overcome the minimum conductivity problem. Furthermore, the sensitivity of electronic structure toward doping makes the graphene a potential material for chemical sensors owing to their exceptionally high surface to volume ratio.

The authors thanks A. H. Castro Neto, B. Uchoa, and E. B. Barros for the valuable discussions. The authors also acknowledge CENAPAD-SP for computer time and financial support from Brazilian agencies CNPq, FAPERGS (Grants Nos. 0511570/05 and 05/2096.2), and FUNCAP (Grant No. 350220/2006-9). S.B. Fagan acknowledges the Brazilian Woman in Science/2006 grant from Loreal/Paris.

*Corresponding author. agsf@fisica.ufc.br

- ¹D. A. Dikin, S. Stankovich, E. J. Zimney, R. D. Piner, G. H. B. Dommett, G. Evmenenko, S. T. Nguyen, and R. S. Ruoff, *Nature (London)* **448**, 457 (2007).
- ²P. R. Wallace, *Phys. Rev.* **71**, 622 (1947).
- ³K. S. Novoselov, D. Jiang, F. Schedin, T. J. Booth, V. V. Khotkevich, S. V. Morozov, and A. K. Geim, *Proc. Natl. Acad. Sci. U.S.A.* **102**, 10451 (2005).
- ⁴K. S. Novoselov, A. K. Geim, S. V. Morozov, D. Jiang, Y. Zhang, S. V. Dubonos, I. V. Grigorieva, and A. A. Firsov, *Science* **306**, 666 (2004).
- ⁵K. S. Novoselov, A. K. Geim, S. V. Morozov, D. Jiang, M. I. Katsnelson, I. V. Grigorieva, S. V. Dubonos, and A. A. Firsov, *Nature (London)* **438**, 197 (2005).
- ⁶Y. Zhang, Y. W. Tan, H. L. Stormer, and P. Kim, *Nature (London)* **438**, 201 (2005).
- ⁷A. K. Geim and K. S. Novoselov, *Nat. Mater.* **6**, 183 (2007).
- ⁸E. W. Hill, A. K. Geim, K. Novoselov, F. Schedin, and P. Black, *IEEE Trans. Magn.* **42**, 2694 (2006).
- ⁹F. Schedin, A. K. Geim, S. V. Morozov, E. W. Hill, P. Blake, M. I. Katsnelson, and K. S. Novoselov, *Nat. Mater.* **6**, 652 (2007).
- ¹⁰N. M. R. Peres, F. Guinea, and A. H. Castro Neto, *Phys. Rev. B* **73**, 125411 (2006).
- ¹¹B. Uchoa and A. H. Castro Neto, *Phys. Rev. Lett.* **98**, 146801 (2007).
- ¹²T. O. Wehling, K. S. Novoselov, S. V. Morozov, E. E. Vdovin, M. I. Katsnelson, A. K. Geim, and A. I. Lichtenstein, *Nano Lett.* **8**, 173 (2008).
- ¹³O. Leenaerts, B. Partoens, and F. M. Peeters, arXiv:0710.1757 (unpublished).
- ¹⁴J. Nilsson, A. H. Castro Neto, F. Guinea, and N. M. R. Peres, *Phys. Rev. B* **76**, 165416 (2007).
- ¹⁵Y.-W. Son, M. L. Cohen, and S. G. Louie, *Phys. Rev. Lett.* **97**, 216803 (2006).
- ¹⁶T. Ohta, A. Bostwick, T. Seyller, K. Horn, and E. Rotenberg, *Science* **313**, 951 (2006).
- ¹⁷S. Y. Zhou, G.-H. Gweon, A. V. Fedorov, P. N. First, W. A. de Heer, D.-H. Lee, F. Guinea, A. H. Castro Neto, and A. Lanzara, *Nat. Mater.* **6**, 770 (2007).
- ¹⁸S. B. Fagan, A. G. Souza Filho, J. Mendes Filho, P. Corio, and M. S. Dresselhaus, *Chem. Phys. Lett.* **406**, 54 (2005).
- ¹⁹P. Hohenberg and W. Kohn, *Phys. Rev.* **136**, B864 (1964).
- ²⁰P. Ordejón, E. Artacho, and J. M. Soler, *Phys. Rev. B* **53**, R10441 (1996).
- ²¹E. Artacho, D. Sanchez-Portal, P. Ordejón, A. García, and J. M. Soler, *Phys. Status Solidi B* **215**, 809 (1999).
- ²²W. Kohn and L. J. Sham, *Phys. Rev.* **140**, A1133 (1965).
- ²³J. P. Perdew, K. Burke, and M. Ernzerhof, *Phys. Rev. Lett.* **77**, 3865 (1996).
- ²⁴N. Troullier and J. L. Martins, *Phys. Rev. B* **43**, 1993 (1991).
- ²⁵L. Kleinman and D. M. Bylander, *Phys. Rev. Lett.* **48**, 1425 (1982).
- ²⁶H. J. Monkhorst and J. D. Pack, *Phys. Rev. B* **13**, 5188 (1976).
- ²⁷F. Valencia, A. H. Romero, F. Ancilotto, and P. L. Silvestrelli, *J. Phys. Chem. B* **110**, 14832 (2006).
- ²⁸S. F. Boys and F. Bernardi, *Mol. Phys.* **19**, 553 (1970).
- ²⁹D. M. Ceperley and B. J. Alder, *Phys. Rev. Lett.* **45**, 566 (1980).